



HAL
open science

Structure and Properties of Dimorphic CePdZn

Rainer Poettgen, Wilfried Hermes, Dirk Johrendt, Helen Müller, Ratikanta Mishra

► **To cite this version:**

Rainer Poettgen, Wilfried Hermes, Dirk Johrendt, Helen Müller, Ratikanta Mishra. Structure and Properties of Dimorphic CePdZn. *Journal of Inorganic and General Chemistry / Zeitschrift für anorganische und allgemeine Chemie*, 2009, 635 (4-5), pp.660. 10.1002/zaac.200900054 . hal-00482073

HAL Id: hal-00482073

<https://hal.science/hal-00482073>

Submitted on 8 May 2010

HAL is a multi-disciplinary open access archive for the deposit and dissemination of scientific research documents, whether they are published or not. The documents may come from teaching and research institutions in France or abroad, or from public or private research centers.

L'archive ouverte pluridisciplinaire **HAL**, est destinée au dépôt et à la diffusion de documents scientifiques de niveau recherche, publiés ou non, émanant des établissements d'enseignement et de recherche français ou étrangers, des laboratoires publics ou privés.

**Structure and Properties of Dimorphic CePdZn**

Journal:	<i>Zeitschrift für Anorganische und Allgemeine Chemie</i>
Manuscript ID:	zaac.200900054
Wiley - Manuscript type:	Article
Date Submitted by the Author:	20-Jan-2009
Complete List of Authors:	Poettgen, Rainer; Westf. Wilhelms-Universitaet, Inst. f. Anorgan. u. Analyt. Chemie Hermes, Wilfried Johrendt, Dirk Müller, Helen Mishra, Ratikanta
Keywords:	cerium, dimorphism



To be submitted to *Z. Anorg. Allg. Chem.*

20.01.09 02:20:20

Structure and Properties of Dimorphic CePdZn

Wilfried Hermes^a, Ratikanta Mishra^{a, b}, Helen Müller^c, Dirk Johrendt^{c, *}, Rainer Pöttgen^{a, *}

^a Münster, Institut für Anorganische und Analytische Chemie der Westfälischen Wilhelms-Universität and NRW Graduate School of Chemistry

^b Mumbai/India, Bhaba Atomic Research Center

^c München, Department Chemie und Biochemie der Ludwig-Maximilians-Universität

Received,

Dedicated to Professor Reinhard Nesper on the occasion of his 60th birthday

Abstract. Two modifications of CePdZn have been synthesized and structurally characterized. The high-temperature (HT) β -CePdZn modification forms upon quenching from the melt. The β -CePdZn structure adopts the orthorhombic TiNiSi type and transforms to the low-temperature (LT) α -CePdZn modification (ZrNiAl type) upon annealing at 1080 K. Both modifications have been studied by X-ray powder and single crystal data: $P6_3/m$, $a = 740.4(1)$, $c = 402.18(5)$ pm, $wR2 = 0.0427$, 237 F^2 values and 14 variables for α -CePdZn and $Pnma$, $a = 707.2(2)$, $b = 441.4(2)$, $c = 806.3(3)$ pm, $wR2 = 0.0827$, 469 F^2 values and 20 variables for β -CePdZn. The palladium and zinc atoms build up three-dimensional [PdZn] networks in both modifications which leave channels for the cerium atoms. Both modifications show stable trivalent cerium. β -CePdZn orders anti-ferromagnetically at 3.2(1) K while no magnetic ordering has been observed for α -CePdZn down to 2 K. The course of the magnetic data points to stronger Ce(4f)–Pd(4d) hybridization in α -CePdZn. Electronic structure calculations reveal only small differ-

ences between α - and β -CePdZn regarding the total energy and the Ce(4f)–Pd(4d) hybridization.

Running title: Structure and Properties of Dimorphic CePdZn

Keywords: Cerium, Crystal Chemistry, Phase Transition

* Prof. Dr. Rainer Pöttgen

Institut für Anorganische und Analytische Chemie, Universität Münster

Corrensstrasse 30, D-48149 Münster, Germany

e-mail: pottgen@uni-muenster.de

Dr. Ratikanta Mishra

Applied Chemistry Division, Bhabha Atomic Research Centre

Trombay, Mumbai-400 085, India

e-mail: mishrar@barc.gov.in

* Prof. Dr. Dirk Johrendt

Department Chemie und Biochemie, Universität München

Butenandtstrasse 5–13 (Haus D), D-81377 München, Germany

e-mail: dirk.johrendt@cup.uni-muenchen.de

Introduction

The equiatomic cerium compounds $CeTX$ (T = late transition metal; X = element of the 3rd, 4th, and 5th main group, Mg, Zn, Cd) have intensively been studied in the last thirty years with respect to their crystal chemistry and greatly varying magnetic and electrical properties, *i.e.* magnetic ordering with high-ordering temperatures, valence fluctuations, heavy-fermion behaviour, Kondo semimetals or semiconductors, non-Fermi liquid behaviour or quantum phase transitions. An important parameter that governs the electronic and magnetic ground states is the hybridization between the 4f(Ce) orbitals and the conduction electrons.

Most of the $CeTX$ structures are superstructures or intergrowth variants which derive from the aristotypes AIB_2 and/or Fe_2P and their structures are stable over a wide temperature range. Recently, for some $CeTX$ structures, structural transitions driven by temperature, pressure, or the cerium valence have been reported. To give some examples, under hydrostatic pressure of 8.7 GPa the germanide CeAuGe shows a first order phase transition from a hexagonal NdPtSb type to an orthorhombic TiNiSi type structure [1].

CePtSn transforms to a ZrNiAl type high-pressure modification under 9.2 GPa and 1325 K [2] and CePdSn [3] shows similar phase transformation. Dimorphism of CePdAl is driven by temperature. The ZrNiAl type high-temperature modification [4] transforms to a low-temperature (LT) modification with a new structure type upon annealing the sample at 1170 K [5]. One of the most interesting compounds is the Kondo insulator CeRhAs [6, 7] which shows three successive temperature driven phase transition associated with a charge-density-wave and two different modulation vectors. The stannide CeRuSn [8] is a static intermediate-valent system which shows trivalent intermediate-valent ordering at room temperature and a transition to a modulated structure at low temperature. The latter is associated with a temperature-driven valence change of cerium.

In the corresponding equiatomic systems with zinc, so far only X-ray powder data of CeTZn ($T = \text{Cu, Ag}$) [9, 10], CeNiZn and CePdZn [11, 12], and single crystal data of CePtZn [13], CeAuZn [12], CeZnGe [14, 15], CeZnSn [16, 17], and CeRhZn [18] have been reported. The nickel and palladium compound crystallize with the hexagonal ZrNiAl type structure while CePtZn adopts the TiNiSi type. For CeCuZn [9, 10] and CeAgZn [9] the orthorhombic KHg₂ type, space group *Imma*, has been reported with a statistical occupancy of the 8h mercury site. Especially for the copper series it is hard to detect the Cu–Zn order by X-ray diffraction since both elements differ by one electron only. CeZnGe and CeZnSn crystallize in the well known YPtAs type structure. CeRhZn [18] adopts the LaNiAl type. In the course of our systematic studies on the magnetic properties of CeTX intermetallics we have re-examined CePdZn. Crystal growth experiments at different temperatures revealed dimorphism with a TiNiSi type high-temperature (HT) modification. Herein we report on the single crystal structure refinements and magnetic properties of both modifications.

Experimental

Synthesis

Starting materials for the synthesis of LT- and HT-CePdZn were a cerium ingot (Johnson Matthey), palladium powder (Degussa-Hüls, ca. 200 mesh), and zinc granules (Merck), all with a stated purity better than 99.9 %. Pieces of the cerium ingot were first

1
2
3
4
5
6 arc-melted [19] into small buttons under purified argon. The argon was purified before
7 with molecular sieves, silica gel and titanium sponge (900 K). The elements were then
8 weighed in the ideal 1:1:1 atomic ratio and arc-welded in small tantalum tubes. The tan-
9 talum ampoules were placed in a water-cooled sample chamber of an induction furnace
10 (Hüttinger Elektronik, Freiburg, Typ TIG 1.5/300) [20], rapidly heated to 1370 K and
11 kept at that temperature for 5 min. The temperature was controlled through a Sensor
12 Therm Metis MS09 pyrometer with an accuracy of ± 30 K. The sample was then
13 quenched by switching off the power supply. This annealing sequence was repeated two
14 times, leading to the TiNiSi type high-temperature modification. The silvery brittle
15 sample could easily be separated from the tantalum tube. No reaction with the container
16 material was evident.
17
18
19
20
21
22
23
24
25

26 For transformation to the low-temperature phase, powder of HT-CePdZn was cold-
27 pressed to a small pellet (\varnothing 6 mm) and placed in a small tantalum crucible in a sealed
28 silica ampoule. The latter was annealed at 1080 K for two weeks. Alternatively LT-
29 CePdZn can be prepared directly from the elements in a tantalum tube in the high-
30 frequency furnace. The sample was first rapidly annealed at 1370 K, followed by an an-
31 nealing sequence of 6 h at 970 K. The much shorter reaction time of the induction melt-
32 ing is due to the higher diffusion rates in the oscillating high-frequency field.
33
34
35
36
37
38
39

40 *X-ray Image Plate Data and Data Collection*

41 All samples were characterized through Guinier powder patterns using $\text{CuK}\alpha_1$ radiation
42 and α -quartz ($a = 491.30$ and $c = 540.46$ pm) as an internal standard. The Guinier cam-
43 era was equipped with a Fujifilm / BAS-1800 image plate system. The lattice param-
44 eters were refined from the powder data (Table 1). The correct indexing was ensured by
45 comparison of the experimental patterns with calculated ones [21] taking the atomic po-
46 sitions obtained from the structure refinement. The experimental patterns are presented
47 in Figure 1. Our powder lattice parameters for LT-CePdZn are in good agreement with
48 the data originally reported by Iandelli ($a = 739.9$, $c = 401.4$ pm) [11].
49
50
51
52
53
54
55
56

57 Irregularly shaped single crystals were selected from both samples by mechanical
58 fragmentation. They were investigated by Laue photographs on a Buerger camera (white
59 molybdenum radiation; imaging plate technique, Fujifilm, BAS-1800) in order to check
60

1
2
3
4
5
6 the quality for intensity data collection. Intensity data of α -CePdZn were collected at
7 room temperature by use of a four-circle diffractometer (CAD4) with graphite mono-
8 chromatized MoK α (71.073 pm) radiation and a scintillation counter with pulse height
9 discrimination. Scans were taken in the $\omega/2\theta$ mode. An empirical absorption correction
10 was applied on the basis of Ψ -scan data, accompanied by a spherical absorption correc-
11 tion. Data of β -CePdZn were collected at room temperature by use of a Stoe IPDS-II
12 image plate system (graphite monochromatized Mo radiation; $\lambda = 71.073$ pm) in oscilla-
13 tion mode and a numerical absorption correction was applied to this data set. All rele-
14 vant crystallographic data and details of the data collections are listed in Table 1.
15
16
17
18
19
20
21

22 The single crystals of α - and β -CePdZn investigated on the diffractometer and the
23 bulk samples were studied by energy dispersive analyses of X-rays (EDX) using a Leica
24 420i scanning electron microscope with CeO₂, palladium, and zinc as standards. The
25 experimentally observed compositions were close to the ideal one and no impurity ele-
26 ments were observed.
27
28
29
30
31

32 ***Physical Property Measurements***

33
34 12.42 and 14.61 mg of the α - and β -CePdZn samples were packed in kapton foil and
35 attached to the sample holder rod of a VSM for measuring the magnetic properties in a
36 Quantum Design Physical-Property-Measurement-System in the temperature range 2.1–
37 305 K with magnetic flux densities up to 80 kOe. For heat capacity (C_p) measurements
38 (2.1–50 K) the samples were glued to the platform of a pre-calibrated heat capacity puck
39 using *Apiezon N grease*.
40
41
42
43
44

45 ***Computational Details***

46
47 The total energies and atomic structure calculations have been performed with the
48 Vienna *ab initio* Simulation Package (VASP) [22], based on density functional theory.
49 The all electron PAW method was used [23] and the cut-off energy for the plane-wave
50 expansion was 375 eV. Convergence limits were 1×10^{-6} eV per formula unit (total en-
51 ergy) and 5×10^{-4} eV \AA^{-1} (forces). Exchange and correlation were treated by the local
52 density approximation (LDA) proposed by Perdew and Zunger [24]. In addition the gen-
53 eralized-gradient approximation (GGA) of Perdew, Burke and Ernzerhof [25] was used.
54
55
56
57
58
59
60 Integration in the Brillouin zone were done by the tetrahedron method including Blöchl

1
2
3
4
5
6 correction [26] using a $6 \times 6 \times 10$ mesh of 42 k points for α -CePdZn and a $5 \times 8 \times 6$
7
8 mesh of 60 k points for β -CePdZn.
9

10 11 **Results and Discussion**

12 13 *Structure Refinements*

14
15 The isotypy of α -CePdZn with the hexagonal ZrNiAl type [27] and β -CePdZn with
16 the orthorhombic TiNiSi type [28] was already evident from the Guinier powder data.
17 Consequently, the diffractometer data sets were in agreement with space groups $P6_3\bar{2}m$
18 (α -CePdZn) and $Pnma$ (β -CePdZn). The atomic positions of NP- and HP-CePdSn [3]
19 were taken as starting atomic parameters and both structures were refined using
20 SHELXL-97 [29] (full-matrix least-squares on F^2) with anisotropic atomic displacement
21 parameters for all atoms. The occupancy parameters were refined in separate series of
22 least-squares cycles in order to check for deviations from the ideal composition. All
23 sites were fully occupied within two standard uncertainties and in the final cycles the
24 ideal occupancy parameters were assumed again. Refinement of the correct absolute
25 structure for α -CePdZn was ensured through calculation of the Flack parameter [30, 31].
26 Final difference Fourier synthesis revealed no significant residual peaks. The positional
27 parameters and interatomic distances are listed in Tables 2 and 3. Further details on the
28 structure refinements are available.*
29
30
31
32
33
34
35
36
37
38
39
40

41
42 * Details may be obtained from: Fachinformationszentrum Karlsruhe, D-76344 Eggen-
43 stein-Leopoldshafen (Germany), by quoting the Registry No's. CSD-420208 (α -
44 CePdZn) and CSD-420207 (β -CePdZn).
45
46
47
48

49 50 *Crystal Chemistry*

51 The structures of the low- and high-temperature modification of CePdZn have been
52 refined from single crystal diffractometer data. So far, only X-ray powder data have
53 been reported for the hexagonal modification by Iandelli [11]. The corresponding struc-
54 ture types ZrNiAl [27] for α -CePdZn and TiNiSi [28] for β -CePdZn have repeatedly
55 been discussed in literature [32-38]. For further details we refer to these overviews and
56
57
58
59
60

the recent work on dimorphic CePtSn [2] and YbPdSn [39, 40]. Herein we focus only on the peculiarities for dimorphic CePdZn.

The cerium near neighbour coordination of α - and β -CePdZn is presented in Figure 2. Both cerium sites have five nearest palladium neighbors. This coordination would have been expected from the course of the electronegativities. In α -CePdZn the average Ce–Pd distance (301.5 pm) is somewhat smaller than in β -CePdZn (307.5 pm) and one can expect stronger Ce(4f)–Pd(4d) hybridization in α -CePdZn, as supported by the magnetic and specific heat data (*vide infra*). The Ce–Pd distances are all slightly longer than the sum of the covalent radii [41] of 293 pm. The Ce–Ce distances in both modifications are well above the Hill limit [42] for f electron localization of 340 pm.

Quantum chemical calculations

The crystal structures of α -CePdZn and β -CePdZn were optimized by using LDA and GGA functionals. The optimized lattice parameters are presented in Table 4. The volume per formula unit calculated for α -CePdZn is slightly smaller than for β -CePdZn in agreement with the experimental data, thus indeed the low temperature modification shows a slightly smaller unit cell volume as the high temperature modification. The calculated total energies (Table 5) of the high and low temperature modifications are almost the same (± 1 kJ/mol) within the LDA (β -CePdZn more stable) and GGA (α -CePdZn more stable), and thus allow no identification of one polymorph to be the most stable. The calculated densities of states (DOS) of α - and β -CePdZn (Figure 6) clearly reveal hybridization of Ce (4-f) and Pd (4-d) states for both modifications. However, the difference of this hybridization is rather small and allows no reliable quantification.

Magnetic susceptibility and specific heat

In the literature only the magnetic properties of CePd₂Zn₃ in the ternary intermetallic Ce–Pd–Zn system have been described so far. CePd₂Zn₃ shows paramagnetic behaviour with stable trivalent cerium and no hint for magnetic ordering was observed down to 2.1 K [43].

The temperature dependence of the magnetic ($\chi = M/H$) and the inverse magnetic susceptibility $\chi^{-1}(T)$ of α -CePdZn and β -CePdZn are displayed in Figure 3, measured

1
2
3
4
5
6 while warming in a *dc* field of 10 kOe after zero field cooling each sample to the lowest
7 available temperature. For both compounds studied here, χ increases with decreasing
8 temperature. Down to 3.1 K, the $H = 10$ kOe susceptibility data give no hint for mag-
9 netic ordering in both modifications. Both compounds show Curie-Weiss behavior in
10 the temperature range 75–300 K. A fit of the susceptibility data in this temperature
11 range revealed an effective magnetic moment of $\mu_{\text{eff}} = 2.42(1) \mu_{\text{B}}/\text{Ce}$ atom and a para-
12 magnetic Curie temperature of $\theta_{\text{P}} = -39.6(1)$ K for α -CePdZn and $\mu_{\text{eff}} = 2.54(1) \mu_{\text{B}}/\text{Ce}$
13 atom and $\theta_{\text{P}} = 3.3(1)$ K for β -CePdZn. These μ_{eff} values are close to the free ion value of
14 $2.54 \mu_{\text{B}}$ for Ce^{3+} , thus indicating purely trivalent cerium in both modifications. The θ_{P}
15 values indicate that the magnetic interaction is of a ferromagnetic type in β -CePdZn and
16 of an antiferromagnetic type in α -CePdZn. β -CePdZn follows almost a Curie law. The
17 deviation of $1/\chi$ vs T in α -CePdZn at low temperatures may be influenced by crystal
18 electric field splitting of the $J = 5/2$ ground state of Ce^{3+} and a thermally induced change
19 of the $4f$ electron level occupancy and/or the beginning of short-range magnetic fluctua-
20 tions, as frequently observed in related cerium intermetallics, *e.g.* CeTPb ($T = \text{Cu, Pd,}$
21 Ag, Au) [44] and CePtZn [13]. It is important to note that the susceptibility χ_{m} (meas-
22 ured at 10 kOe) of β -CePdZn at 3 K is almost four times larger than that determined for
23 α -CePdZn. In other words, the magnetic correlations in β -CePdZn are enhanced. An
24 anomaly at around 3.4(1) K is clearly visible for the high temperature modification in
25 the $\chi(T)$ curve measured at a low field of 100 Oe (inset of Figure 3). Both the ZFC and
26 the FC data show an antiferromagnetic transition at $T_{\text{N}} = 3.4(1)$ K, they do not bifurcate
27 and are the same within the experimental errors. For α -CePdZn we could not observed a
28 magnetic transition down to 2.1 K measured at a low field of 100 Oe.

29
30
31
32
33
34
35
36
37
38
39
40
41
42
43
44
45
46
47
48 Due to the abased susceptibility in α -CePdZn, the smaller value of μ_{eff} in α -CePdZn,
49 the observed antiferromagnetic ordering at 3.4(1) K in β -CePdZn and no ordering in α -
50 CePdZn, we can establish an increase of the J_{cf} interaction from the high temperature
51 modification to the low temperature modification, enabling stronger Ce ($4f$)–Pd ($4d$)
52 hybridization. This is in line with the crystal chemical data (*vide ultra*).

53
54
55
56
57
58 In Figure 4 we present the magnetization data for α -CePdZn and β -CePdZn measured
59 in ZFC state at 5, 10 and 15 K. The magnetizations for α -CePdZn and β -CePdZn vary
60

1
2
3
4
5
6 almost in a linear fashion at 10 and 15 K as expected for a paramagnetic material. At 5
7 K the curvature becomes more pronounced for both samples, but stronger for the high-
8 temperature modification. β -CePdZn shows a tendency for saturation at high fields. M
9 ($T = 5$ K) varies linearly with initial application of the field and reveals a curvature
10 above 20 kOe, clearly indicating the antiferromagnetic nature of magnetic ordering in β -
11 CePdZn. It may be noted here that, for both modifications, the maximum moment ob-
12 served at 80 kOe and 5 K does not reach the expected moment value of $2.14 \mu_B / \text{Ce}$
13 atom (according to $g \times J$). The values for α -CePdZn and β -CePdZn are 0.4 and 1.2
14 μ_B/Ce atom, respectively. The decrease in the saturation moment can be attributed to
15 crystal field effects (see also the deviation of $\chi^{-1}(T)$ from the Curie-Weiss fit, especially
16 in α -CePdZn), and has been observed for many other cerium intermetallics [45, 46, and
17 refs. therein]. The smaller value of the observed moment in α -CePdZn is in line with a
18 stronger Ce ($4f$)–Pd ($4d$) hybridization, in agreement with the structural data (*vide ul-*
19 *tra*).
20
21
22
23
24
25
26
27
28
29
30

31
32 The specific heat (C_p) data are plotted in Fig. 5. The magnetic ordering temperature
33 (Néel temperature) of β -CePdZn is characterized by a λ -like anomaly. The ordering
34 temperature is 3.2(1) K, in good agreement with the magnetic data. α -CePdZn does not
35 order magnetically above 2.1 K.
36
37
38
39

40 We thank Dipl.-Ing. U. Ch. Rodewald for the intensity data collections. This work was finan-
41 cially supported by the Deutsche Forschungsgemeinschaft. R.M. is indebted to the Alexander-
42 von-Humboldt Foundation for a research stipend. The PhD thesis of W.H. is supported by the
43 Fonds der Chemischen Industrie.
44
45
46
47

48 References

- 49
50 [1] V. Brouskov, M. Hanfland, R. Pöttgen, U. Schwarz, *Z. Kristallogr.* **2005**, *220*,
51 122.
52 [2] J. F. Riecken, G. Heymann, T. Soltner, R.-D. Hoffmann, H. Huppertz, D.
53 Johrendt, R. Pöttgen, *Z. Naturforsch.* **2005**, *60b*, 821.
54 [3] G. Heymann, J. F. Riecken, S. Rayaprol, S. Christian, R. Pöttgen, H. Huppertz, *Z.*
55 *Anorg. Allg. Chem.* **2007**, *633*, 77.
56 [4] F. Hulliger, *J. Alloys Compd.* **1995**, *218*, 44.
57
58
59
60

- 1
2
3
4
5
6 [5] A. Griбанov, A. Tursina, E. Murashova, Y. Seropegin, E. Bauer, H. Kaldarar, R.
7 Lackner, H. Michor, E. Royanian, M. Reissner, P. Rogl, *J. Phys.: Condens. Matter*
8 **2006**, *18*, 9593.
9
10 [6] T. Sasakawa, T. Suemitsu, T. Takabatake, Y. Bando, K. Uemo, M. H. Jung, M.
11 Sera, T. Suzuki, T. Fujita, M. Nakajima, K. Iwasa, M. Kohgi, Ch. Paul, St. Berger,
12 E. Bauer, *Phys. Rev. B* **2002**, *66*, 041103.
13
14 [7] K. Uemo, K. Masumori, T. Sasakawa, F. Iga, T. Takabatake, Y. Ohishi, T.
15 Adachi, *Phys. Rev. B* **2005**, *71*, 064110.
16
17 [8] J. F. Riecken, W. Hermes, B. Chevalier, R.-D. Hoffmann, F. M. Schappacher, R.
18 Pöttgen, *Z. Anorg. Allg. Chem.* **2007**, *633*, 1094.
19
20 [9] M. L. Fornasini, A. Iandelli, F. Merlo, M. Pani, *Intermetallics*, **2000**, *8*, 239.
21
22 [10] P. Morin, D. Gignoux, J. Voiron, A. P. Murani, *Physica B*, **1992**, *180&181*, 173.
23
24 [11] A. Iandelli, *J. Alloys Compd.* **1992**, *182*, 87.
25
26 [12] W. Hermes, R. Mishra, U. Ch. Rodewald, R. Pöttgen, *Z. Naturforsch.*, **2008**, *63b*,
27 537.
28
29 [13] R. Mishra, W. Hermes, R. Pöttgen, *Z. Naturforsch.* **2007**, *62b*, 1581.
30
31 [14] M. Pani, P. Manfrinetti, A. Palenzona, *Intermetallics*, **2009**, *17*, ###.
32 Doi:10.1016/j.intermet.2008.10.008
33
34 [15] W. Hermes, R. Pöttgen, *Z. Naturforsch.* **2009**, *64b*, in press.
35
36 [16] P. Manfrinetti, M. Pani, *J. Alloys Compd.* **2005**, *393*, 180.
37
38 [17] W. Hermes, S. F. Matar, T. Harmening, U. Ch. Rodewald, M. Eul, R. Pöttgen, *Z.*
39 *Naturforsch.* **2009**, *64b*, in press.
40
41 [18] W. Hermes, A. F. Al Alam, S. F. Matar, R. Pöttgen, *Solid State Sci.*, **2008**, *10*,
42 1895.
43
44 [19] R. Pöttgen, Th. Gulden, A. Simon, *GIT Labor Fachzeitschrift* **1999**, *43*, 133.
45
46 [20] D. Kußmann, R.-D. Hoffmann, R. Pöttgen, *Z. Anorg. Allg. Chem.* **1998**, *624*,
47 1727.
48
49 [21] K. Yvon, W. Jeitschko, E. Parthé, *J. Appl. Crystallogr.* **1977**, *10*, 73.
50
51 [22] G. Kresse, J. Furthmüller, *Comput. Mater. Sci.* **1996**, *6*, 15.
52
53 [23] G. Kresse, D. Joubert, *Phys. Rev. B* **1999**, *59*, 1758.
54
55 [24] J. P. Perdew, A. Zunger, *Phys. Rev. B* **1981**, *23*, 5048.
56
57 [25] J. P. Perdew, S. Burke, M. Ernzerhof, *Phys. Rev. Lett.* **1996**, *77*, 3865.
58
59 [26] P. E. Blöchl, *Phys. Rev. B* **1994**, *50*, 17953.
60
[27] M. F. Zumdick, R.-D. Hoffmann, R. Pöttgen, *Z. Naturforsch.* **1999**, *54b*, 45.
[28] C. B. Shoemaker, D. P. Shoemaker, *Acta Crystallogr.* **1965**, *18*, 900.

- 1
2
3
4
5
6 [29] G. M. Sheldrick, SHELXL-97 – *Program for Crystal Structure Refinement*, University of Göttingen, Germany **1997**.
- 7
8
9 [30] H. D. Flack, G. Bernadinelli, *Acta Crystallogr. A* **1999**, *55*, 908.
- 10 [31] H. D. Flack, G. Bernadinelli, *J. Appl. Crystallogr.* **2000**, *33*, 1143.
- 11 [32] G. Nuspl, K. Polborn, J. Evers, G. A. Landrum, R. Hoffmann, *Inorg. Chem.* **1996**,
12 *35*, 6922.
- 13 [33] G. A. Landrum, R. Hoffmann, J. Evers, H. Boysen, *Inorg. Chem.* **1998**, *37*, 5754.
- 14 [34] R.-D. Hoffmann, R. Pöttgen, *Z. Kristallogr.* **2001**, *216*, 127.
- 15 [35] M. D. Bojin, R. Hoffmann, *Helv. Chim. Acta* **2003**, *86*, 1653.
- 16 [36] M. D. Bojin, R. Hoffmann, *Helv. Chim. Acta* **2003**, *86*, 1683.
- 17 [37] E. Parthé, L. Gelato, B. Chabot, M. Penzo, K. Cenzual, R. Gladyshevskii, TYPIX–
18 Standardized Data and Crystal Chemical Characterization of Inorganic Structure
19 Types. Gmelin Handbook of Inorganic and Organometallic Chemistry, 8th edition,
20 Springer, Berlin (Germany) **1993**.
- 21 [38] M. F. Zumdick, R. Pöttgen, *Z. Kristallogr.* **1999**, *214*, 90.
- 22 [39] D. Kußmann, R. Pöttgen, B. Künnen, R. Müllmann, B. D. Mosel, G. Kotzyba, *Z.*
23 *Kristallogr.* **1998**, *613*, 356.
- 24 [40] T. Görlach, S. Putselyk, A. Hamann, T. Tomanić, M. Uhlarz, F. M. Schappacher,
25 R. Pöttgen, H. v. Löhneysen, *Phys. Rev. B* **2007**, *76*, 205112.
- 26 [41] J. Emsley, *The Elements*, Oxford University Press, Oxford (U.K.) **1999**.
- 27 [42] H. H. Hill, in *Plutonium and other Actinides*, Mines, W. N. (ed.) *Nuclear Materi-*
28 *als Series, AIME* **1970**, *17*, 2.
- 29 [43] W. Hermes, St. Linsinger, R. Mishra, R. Pöttgen, *Monatsh. Chem.* **2008**, *139*,
30 1143.
- 31 [44] W. Hermes, S. Rayaprol, R. Pöttgen, *Z. Naturforsch.* **2007**, *62b*, 901.
- 32 [45] R. Kraft, R. Pöttgen, D. Kaczorowski, *Chem. Mater.* **2003**, *15*, 2998.
- 33 [46] R. Movshovich, J. M. Lawrence, M. F. Hundley, J. Neumeier, J. D. Thompson, A.
34 Lacerda, Z. Fisk, *Phys. Rev. B* **1996**, *53*, 5456.
- 35
36
37
38
39
40
41
42
43
44
45
46
47
48
49
50
51
52
53
54
55
56
57
58
59
60

Table 1. Crystal data and structure refinement for α - and β -CePdZn.

Empirical formula	α -CePdZn	β -CePdZn
	low-temperature phase	high-temperature phase
Molar mass	311.89 g/mol	311.89 g/mol
Space group; <i>Z</i>	$P6_3\bar{2}m$; 3	$Pnma$; 4
Structure type	ZrNiAl	TiNiSi
Pearson symbol	hP9	oP12
Unit cell dimensions (Guinier powder data)	$a = 740.4(1)$ pm $b = a$ $c = 402.18(5)$ pm $V = 0.1909$ nm ³	$a = 707.2(2)$ pm $b = 441.4(2)$ pm $c = 806.3(3)$ pm $V = 0.2517$ nm ³
Calculated density	8.14 g/cm ³	8.23 g/cm ³
Crystal size	30 × 40 × 50 μ m ³	20 × 30 × 60 μ m ³
Transm. ratio (max/min)	1.20	5.76
Absorption coefficient	33.5 mm ⁻¹	33.9 mm ⁻¹
F(000)	402	536
θ Range	3 to 30°	3 to 32°
Range in hkl	± 10 ; ± 10 ; 0–5	± 10 ; ± 6 ; ± 11
Total no. reflections	1259	5816
Independent reflections	237 ($R_{\text{int}} = 0.1081$)	469 ($R_{\text{int}} = 0.1259$)
Reflections with $I > 2\sigma(I)$	205 ($R_{\text{sigma}} = 0.0552$)	400 ($R_{\text{sigma}} = 0.0448$)
Data / parameters	237 / 14	469 / 20
Goodness-of-fit on F^2	1.092	1.063
Final <i>R</i> indices [$I > 2\sigma(I)$]	$R_1 = 0.0315$ $wR_2 = 0.0400$	$R_1 = 0.0332$ $wR_2 = 0.0816$
<i>R</i> indices (all data)	$R_1 = 0.0442$ $wR_2 = 0.0427$	$R_1 = 0.0382$ $wR_2 = 0.0827$
Extinction coefficient	0.0039(5)	0.009(1)
Flack parameter	0.11(7)	–
Largest diff. peak and hole	1.62 / –1.58 e/Å ³	2.59 / –3.84 e/Å ³

Table 2. Atomic coordinates and anisotropic displacement parameters (pm^2) for α - and β -CePdZn. U_{eq} is defined as one third of the trace of the orthogonalized U_{ij} tensor. The anisotropic displacement factor exponent takes the form $-2\pi^2[(ha^*)^2U_{11}+\dots+2kha^*b^*U_{12}]$. $U_{23} = 0$.

Atom	Wyckoff position	x	y	z	U_{11}	U_{22}	U_{33}	U_{12}	U_{13}	U_{eq}
α-CePdZn (low-temperature phase)										
Ce	3 <i>f</i>	0.4113(2)	0	0	108(4)	97(6)	97(5)	48(3)	0	102(3)
Pd1	1 <i>a</i>	0	0	0	151(8)	U_{11}	128(15)	76(4)	0	144(6)
Pd2	2 <i>d</i>	2/3	1/3	1/2	133(6)	U_{11}	106(11)	67(3)	0	124(4)
Zn	3 <i>g</i>	0.7616(3)	0	1/2	133(11)	125(12)	138(13)	62(6)	0	133(6)
β-CePdZn (high-temperature phase)										
Ce	4 <i>c</i>	0.03202(7)	1/4	0.69327(7)	150(3)	138(3)	145(3)	0	-8(2)	144(2)
Pd	4 <i>c</i>	0.26896(10)	1/4	0.39212(10)	166(3)	130(3)	164(4)	0	13(2)	153(2)
Zn	4 <i>c</i>	0.65160(16)	1/4	0.43125(16)	199(5)	133(5)	137(6)	0	-12(4)	156(3)

Table 3. Interatomic distances (pm), calculated with the powder lattice parameters of α - and β -CePdZn. Standard deviations are all equal or less than 0.2 pm. All distances of the first coordination sphere are listed.

α-CePdZn				β-CePdZn			
Ce:	4	Pd2	300.7	Ce:	1	Pd	295.0
	1	Pd1	304.5		2	Pd	307.0
	2	Zn	328.2		2	Pd	314.3
	4	Zn	332.5		1	Zn	314.3
	4	Ce	387.3		2	Zn	320.0
	2	Ce	402.2		2	Zn	329.9
					1	Zn	342.1
					2	Ce	365.3
					1	Pd	382.6
					2	Ce	384.6
Pd1:	6	Zn	267.6	Pd:	2	Zn	268.6
	3	Ce	304.5		1	Zn	272.4
Pd2:	3	Zn	288.4		1	Zn	273.6
	6	Ce	300.7		1	Ce	295.0
					2	Ce	307.0
					2	Ce	314.3
					1	Ce	382.6
Zn:	2	Pd1	267.6	Zn:	2	Pd	268.6
	2	Pd2	288.4		1	Pd	272.4
	2	Zn	305.8		1	Pd	273.6
	2	Ce	328.2		1	Ce	314.3
	4	Ce	332.5		2	Ce	320.0
					2	Zn	327.1
					2	Ce	329.9
					1	Ce	342.1

Table 4. Experimental and theoretical lattice parameters of α - and β -CePdZn.

α-CePdZn			β-CePdZn		
Experiment	LDA	GGA	Experiment	LDA	GGA

volume (nm ³)	0.1909	0.1726	0.1895	0.2517	0.2278	0.2503
<i>a</i> (pm)	740.4(1)	701.95	735.42	707.2(2)	666.86	699.06
<i>b</i> (pm)	<i>b</i> = <i>a</i>	<i>b</i> = <i>a</i>	<i>b</i> = <i>a</i>	441.4(2)	437.19	442.96
<i>c</i> (pm)	402.18(5)	404.59	404.61	806.3(3)	781.37	808.45

Table 5. Total energies per formula unit of α - and β -CePdZn.

	LDA	GGA
α -CePdZn (kJ/mol)	-1639.03	-1393.50
β -CePdZn (kJ/mol)	-1640.02	-1392.33
ΔE (kJ/mol)	0.99	-1.17

Figure Captions

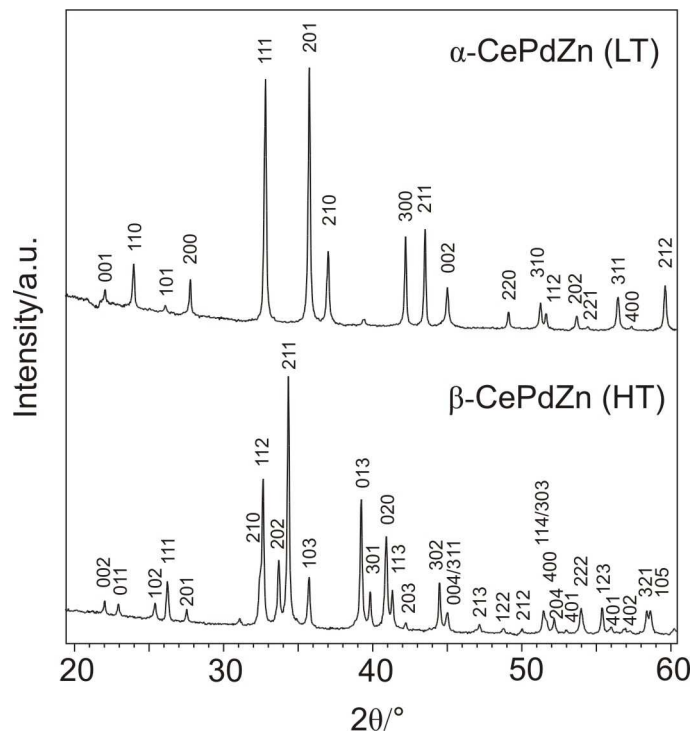


Fig. 1 Guinier powder patterns ($\text{CuK}\alpha_1$ radiation) of α -CePdZn (LT) and β -CePdZn (HT). The hkl indices are indicated.

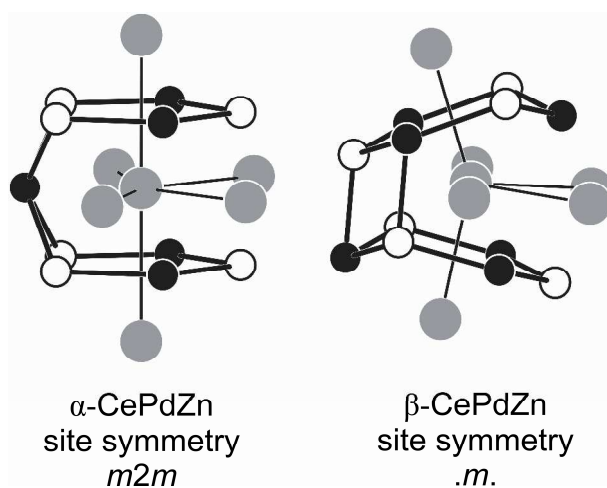


Fig. 2 Coordination polyhedra of the cerium atoms in α - and β -CePdZn. The cerium, palladium, and zinc atoms are drawn as medium grey, filled, and open circles, respectively.

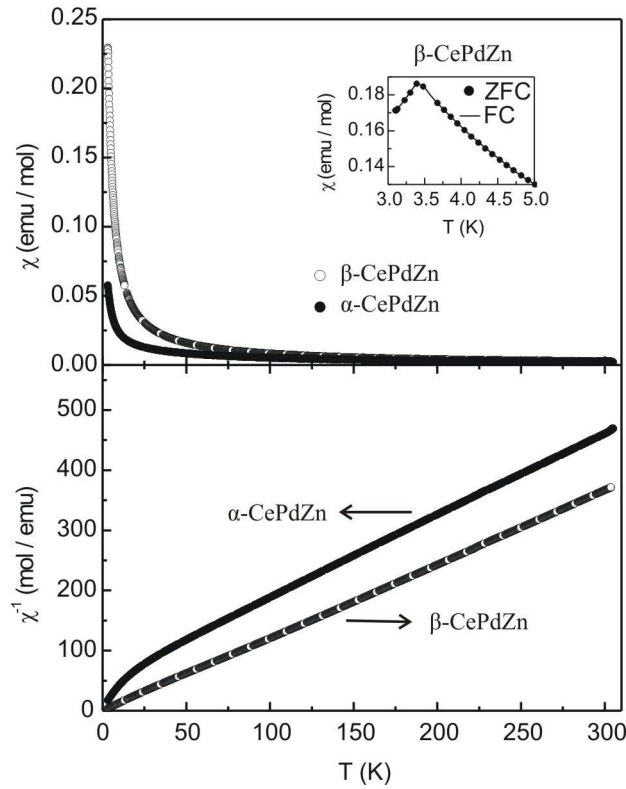


Fig. 3 Temperature dependence of the magnetic (χ) (top panel) and the inverse magnetic susceptibility (χ^{-1}) (bottom panel) of α -CePdZn and β -CePdZn measured at an external flux density of 10 kOe. The inset shows $\chi(T)$ for β -CePdZn measured at $H = 100$ Oe after zero field cooling (ZFC) and field cooling (FC) the sample.

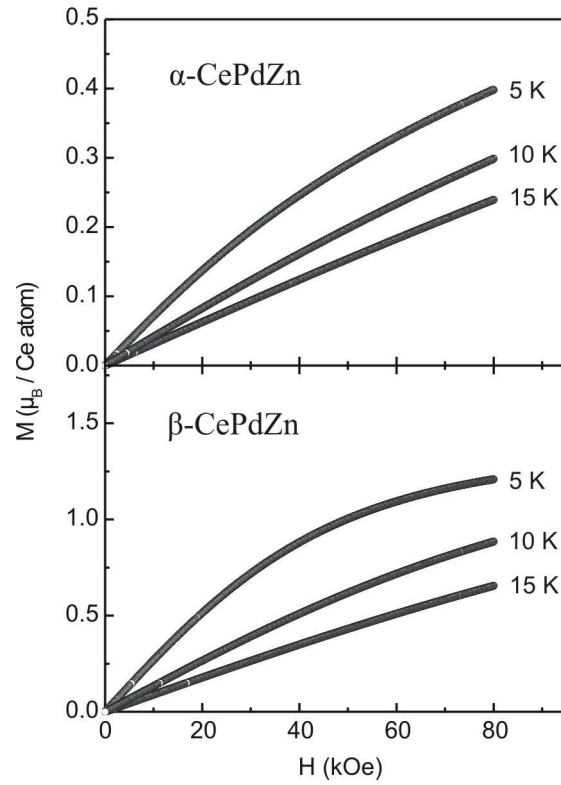


Fig. 4 Magnetization vs external magnetic flux density of α -CePdZn and β -CePdZn at 5, 10, and 15 K.

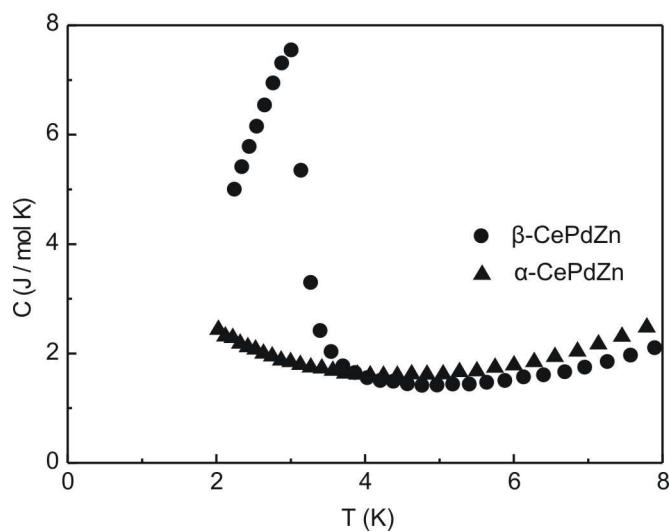


Fig. 5 Temperature dependence of the specific heat of α -CePdZn and β -CePdZn measured in zero magnetic field.

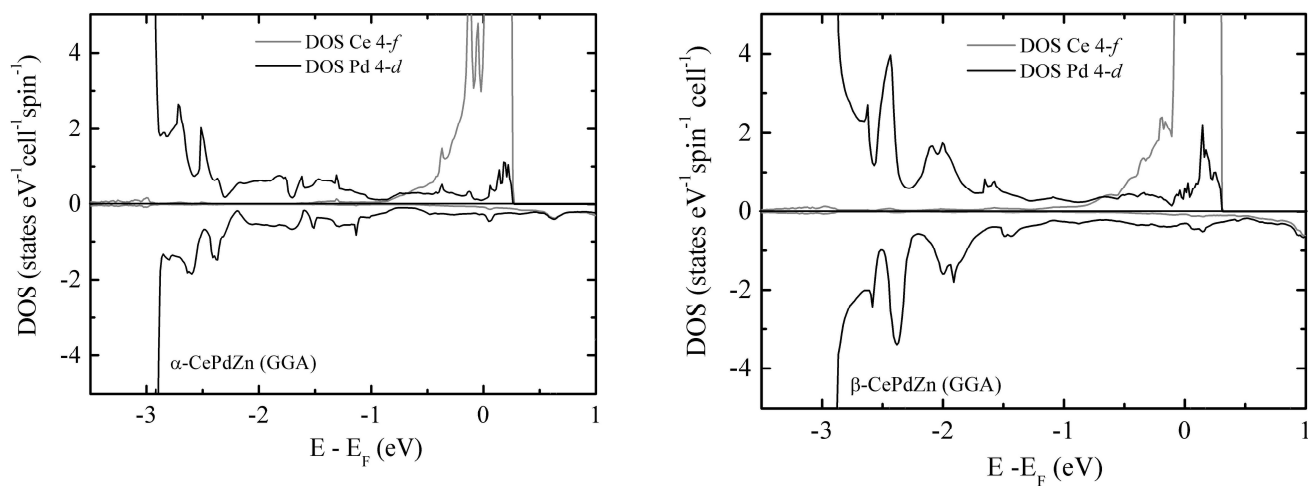


Fig. 6 Density of States for α -CePdZn and β -CePdZn (GGA).